

Oxetane Substrates of Human Microsomal Epoxide Hydrolase[§]

Francesca Toselli, Marlene Fredenwall, Peder Svensson, Xue-Qing Li, Anders Johansson, Lars Weidolf, and Martin A. Hayes

Cardiovascular and Metabolic Diseases, Innovative Medicines and Early Development, AstraZeneca, Mölndal, Sweden (F.T., M.F., X.-Q.L., A.J., L.W., M.A.H.); and Integrative Research Laboratories, Arvid Wallgrens Backe 20, Gothenburg, Sweden (P.S.)

Received April 24, 2017; accepted June 5, 2017

ABSTRACT

Oxetanyl building blocks are increasingly used in drug discovery because of the improved drug-like properties they confer on drug candidates, yet little is currently known about their biotransformation. A series of oxetane-containing analogs was studied and we provide the first direct evidence of oxetane hydrolysis by human recombinant microsomal epoxide hydrolase (mEH). Incubations with human liver fractions and hepatocytes were performed with and without inhibitors of cytochrome P450 (P450), mEH and soluble epoxide hydrolase (sEH). Reaction dependence on NADPH was investigated in subcellular fractions. A full kinetic characterization of oxetane hydrolysis is presented, in both human liver microsomes and human recombinant mEH. In human liver fractions and hepatocytes, hydrolysis by mEH was the only oxetane ring-opening metabolic route, with no contribution

from sEH or from cytochrome P450-catalyzed oxidation. Minimally altering the structural elements in the immediate vicinity of the oxetane can greatly modulate the efficiency of hydrolytic ring cleavage. In particular, higher pK_a in the vicinity of the oxetane and an increased distance between the oxetane ring and the benzylic nitrogen improve reaction rate, which is further enhanced by the presence of methyl groups near or on the oxetane. This work defines oxetanes as the first nonepoxide class of substrates for human mEH, which was previously known to catalyze the hydrolytic ring opening of electrophilic and potentially toxic epoxide-containing drugs, drug metabolites, and exogenous organochemicals. These findings will be of value for the development of biologically active oxetanes and may be exploited for the biocatalytic generation of enantiomerically pure oxetanes and diols.

Introduction

Oxetane rings are becoming widely incorporated in novel drug design because of the improved properties that they confer on drug candidates (Wuitschik et al., 2010; Bull et al., 2016). The use of oxetanyl groups as alternatives to, e.g., gem-dimethyl groups leads to a significant increase in solubility and lower lipophilicity while maintaining steric bulk. The introduction of the spiro-oxetanylazetidiny moiety has also been pursued as a means of providing favorable physicochemical and pharmacokinetic properties compared with larger ring systems (Wuitschik et al., 2010; Bull et al., 2016) and was recently reported in the discovery of the melanin-concentrating hormone receptor antagonist AZD1979 (3-(4-(2-Oxa-6-azaspiro[3.3]heptan-6-ylmethyl)phenoxy)-azetidiny-1-yl)(5-(4-methoxyphenyl)-1,3,4-oxadiazol-2-yl)methanone (Supplemental Fig. 1) (Johansson et al., 2016). In subsequent studies using selective inhibitors in human liver fractions, hydrolytic ring opening of the spiro-oxetanyl ring system in this compound was observed and found to be a novel reaction catalyzed by the human microsomal epoxide hydrolase (mEH) (Li et al., 2016).

mEH (EC 3.3.2.9) is a highly conserved drug-metabolizing enzyme and a member of the α/β -hydrolase fold family of proteins (Morisseau

and Hammock, 2005; Václavíková et al., 2015). mEH is widely expressed in the human body and typically catalyzes the hydrolytic ring opening of epoxide-containing exogenous organochemicals, thus playing an important role in the detoxification of electrophilic and potentially toxic drugs and drug metabolites (Morisseau and Hammock, 2005; Václavíková et al., 2015).

For the continued development of oxetane-containing drug candidates, knowledge on the enzymology of their metabolism is crucial to predict drug-drug interaction risk, model drug exposure in a variety of patient populations, and fulfill regulatory requirements. The objective of the present study was to investigate simple oxetanyl analogs of (3-(4-(2-Oxa-6-azaspiro[3.3]heptan-6-ylmethyl)phenoxy)azetidiny-1-yl)(5-(4-methoxyphenyl)-1,3,4-oxadiazol-2-yl)methanone and to probe the influence on metabolic ring opening of different structural features in the vicinity of the oxetanyl ring. It is shown that oxetanes are exclusively ring opened via hydrolysis by human mEH and that several structural variations in the vicinity of the oxetane greatly affect the rate of hydrolysis. Oxetane hydrolysis by human recombinant mEH, with full kinetic parameters, is also reported, providing the first direct evidence of this new activity of human mEH. This work describes a new class of substrates for this important enzyme and defines hydrolysis as a major metabolic ring-opening pathway for oxetanes.

Materials and Methods

Materials. Pooled, mixed-gender human liver microsomes (HLMs) were purchased from BD Biosciences (Bedford, MA). Pooled, mixed-gender human

This work was presented in preliminary form at the 21st International Symposium on Microsomes and Drug Oxidations; 2016 Oct 2-6, Davis, CA.

<https://doi.org/10.1124/dmd.117.076489>

[§]This article has supplemental material available at dmd.aspetjournals.org.

ABBREVIATIONS: 1-ABT, 1-aminobenzotriazole; cSO, *cis*-stilbene oxide; DMSO, dimethylsulfoxide; 11,12-EET, (\pm)11,12-epoxy-5Z,8Z,14Z-eicosatrienoic acid; EH, epoxide hydrolase; HLC, human liver cytosol; HLM, human liver microsome; KTZ, ketoconazole; mEH, microsomal epoxide hydrolase; MS, mass spectrometry; P450, cytochrome P450; PRG, progabide; Q-TOF, quadrupole time-of-flight; sEH, soluble epoxide hydrolase; *t*-AUCB, *trans*-4-[4-(1-adamantylcarbamoylamino)cyclohexyloxy]benzoic acid; UHPLC, ultra-high-performance liquid chromatography; VPD, valpromide.

liver cytosol (HLC) and cryopreserved hepatocytes were purchased from Bioreclamation IVT (Frankfurt am Main, Germany). Recombinant human mEH was a generous gift from Dr. B. D. Hammock (University of California Davis, Davis, CA). Ketoconazole (KTZ), 1-aminobenzotriazole (1-ABT), progabide (PRG) and *trans*-4-[4-(1-adamantylcarbamoylamino)cyclohexyloxy]benzoic acid (*t*-AUCB) were obtained from AstraZeneca Compound Management (AstraZeneca R&D Gothenburg, Sweden). Valpromide (VPD), styrene oxide, *cis*-stilbene oxide (*c*SO), hydrobenzoin (the product of *c*SO ring opening), bovine serum albumin, and NADPH were purchased from Sigma Aldrich (St. Louis, MO), and (\pm)11,12-Epoxy-5Z,8Z,14Z-eicosatrienoic acid (11,12-EET) was purchased from Cayman Chemicals (Ann Arbor, MI). Oxetanes 1–9 and 15–20, and diols 10–14, 21, and 22 were synthesized and characterized at Medicinal Chemistry, Cardiovascular and Metabolic Diseases, Innovative Medicines and Early Development Biotech Unit, AstraZeneca (Gothenburg, Sweden), as detailed in the Supplemental Material. All other chemicals were of the highest quality commercially available.

Incubations with Human Liver Subcellular Fractions and Selective Inhibitors. The contribution of different liver enzymes to the metabolism of compounds 1–9 and 15–20 (see Tables 1 and 2 for structures) was monitored in HLMs and HLC in the presence of inhibitors. *c*SO and 11,12-EET were used in parallel incubations as positive controls for metabolism by mEH and soluble epoxide hydrolase (sEH), respectively (Chacos et al., 1983; Gill et al., 1983a). The following inhibitors were used (final concentrations): KTZ [cytochrome P450 (P450) inhibitor; 200 μ M], VPD (mEH inhibitor; 10–1000 μ M), or PRG (mEH inhibitor; 100 μ M), in HLMs; and VPD (200 μ M) or *t*-AUCB (sEH inhibitor; 20 μ M), in HLC. Concentrations of all inhibitors were chosen to be in excess of their inhibition constants reported in the literature (Kerr et al., 1989; Kroetz et al., 1993; Emoto et al., 2003; Liu et al., 2009); at the concentration used, KTZ was expected to inhibit all major liver P450s (Emoto et al., 2003).

Compounds 1–9 (10 μ M) or *c*SO (100 μ M) were incubated individually with either HLMs or HLC (1 mg protein/ml) in sodium phosphate buffer (0.1 M, pH 7.4, 50 μ l) for 1 hour at 37°C with constant shaking. Compounds 15–20 were incubated in the same manner, but only with HLMs, whereas 11,12-EET (10 μ M) was incubated only with HLC. The subcellular fractions were preincubated in

buffer with or without NADPH (1 mM) plus inhibitor or vehicle for 3 minutes, and then reactions were started by the addition of substrate. Chemical stability of compounds 1–9 and 15–20 in buffer was also assessed in similar incubations, lacking the liver fractions and the inhibitors. Final solvent concentrations were kept constant in all reactions and were \leq 0.3% (v/v) acetonitrile and \leq 1.1% (v/v) dimethylsulfoxide (DMSO); incubations with PRG and matching controls also contained 0.5% (v/v) methanol; incubations in HLC with 11,12-EET also contained 1.6% (v/v) ethanol. All assays were performed in duplicate, in round-bottom 96-well plates.

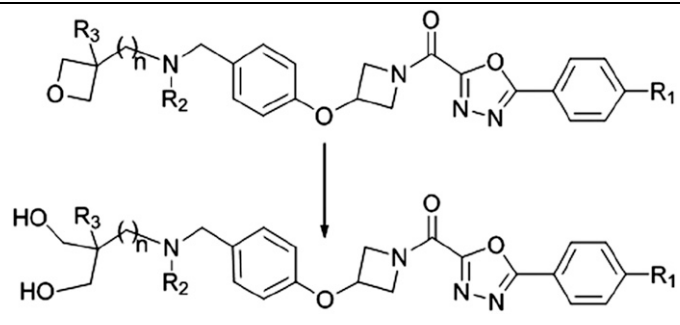
Reactions were quenched by mixing with either one (*c*SO) or three (1–9, 15–20, and 11,12-EET) volumes of ice-cold acetonitrile. After centrifugation at 4000g for 20 minutes, 50 μ l of the supernatant was mixed with an equal volume of water, and the resulting mixture was analyzed by either ultra-high-performance liquid chromatography (UHPLC)/quadrupole time-of-flight (Q-TOF) mass spectrometry (MS) (1–9, 15–20, and 11,12-EET) or UHPLC/UV (*c*SO), as described in detail subsequently.

Incubations with Human Hepatocytes. The metabolism of 1–9, 15–20, and *c*SO was also assessed in human hepatocytes, with or without inhibitors. Inhibitors used were (final concentrations): 1-ABT (P450 inhibitor; 1–2 mM), VPD (100–200 μ M) or *t*-AUCB (10–20 μ M). At the concentrations used, 1-ABT was expected to inhibit strongly all major liver P450s (Emoto et al., 2003).

Cryopreserved hepatocytes were thawed and resuspended in Leibovitz's L-15 medium to a final concentration of 10⁶ cells/ml. Cells were preincubated for 7 minutes at 37°C with inhibitor or vehicle under constant shaking, and reactions were then initiated by the addition of substrate (4 μ M). Chemical stability of substrates in Leibovitz's L-15 medium was assessed in similar incubations, lacking hepatocytes and inhibitors. Final solvent concentrations were 0.04% DMSO and 0.08% acetonitrile in all reactions, and incubations (50 μ l) were performed in duplicate, in flat-bottom 96-well plates. Reactions were quenched after 2 hours and processed as described previously for incubations with subcellular fractions.

Determination of Kinetic Constants for Oxetane Hydrolysis. Human recombinant mEH and HLMs were used to examine the kinetics of oxetane hydrolysis. Conditions for linear product formation with respect to time and

TABLE 1
Physicochemical properties of compounds 1–9 and percentage of dihydrodiol metabolites formed in incubations with HLMs



Compound	R ₁	R ₂	R ₃	n	Solubility ^a	Log D ^a	pK _a ^a	Average % Diol in HLMs (Replicate 1, Replicate 2) ^b
					μ M			
1	MeO	Me	H	0	11	3.0	6.1	0 (0, 0)
2	H	H	H	0	106	2.1	6.6	1.1 (1.2, 0.9)
3	MeO	H	H	0	63	2.2	6.6	1.6 (1.6, 1.7)
4	H	H	Me	1	858	2.3	8.4	15 (15, 15)
5	MeO	H	Me	1	NA	2.0	8.2	16 (16, 16)
6	H	Me	Me	1	80	4	8.5	91 (89, 92)
7	MeO	Me	Me	1	70	4.1	8.0	89 (88, 89)
8	MeO	H	H	1	NA	1.3	NA	2.7 (2.7, 2.8)
9	MeO	H	Me	0	NA	2.3	6.9	<1

NA, not available.

^aSolubility, log D_{7.4} HPLC and pK_a were measured as described previously (Boström et al., 2012).

^bDiol levels were determined from duplicate incubations (60 minutes) of 10 μ M substrate with HLMs, without NADPH. Diol metabolite levels are expressed as a percentage of the sum of parent + diol peak areas.

TABLE 2
 Physicochemical properties of compounds 15–20 and percentage of dihydrodiol metabolites formed in incubations with HLMs

Compound	R ₁	R ₂	R ₃	n	Solubility ^a	Log D ^a	pK _a ^b	Average % Diol in HLMs (Replicate 1, Replicate 2) ^c
					<i>μM</i>			
15	Me	Me	Me	1	258	1.6	8.2	9.9 (10.0, 9.9)
16	Me	Me	Me	1	586	0.4	9.3	1.5 (0, 3.1)
17		Me	Me	1	950	0.8	8.2	2.3 (2.1, 2.5)
18	Me	Me	Me	2	612	1.6	8.9	3.1 (3.0, 3.1)
19	Me	H	Me	2	628	0.5	9.7	0.7 (0.7, 0.7)
20	Me	Me	H	2	587	1.0	8.9	0 (0, 0)

^aSolubility and logD_{7.4} HPLC were measured as described previously (Boström et al., 2012).

^bCalculated values.

^cDiol levels were determined from duplicate incubations (60 minutes) of 10 μM substrate with HLMs, without NADPH. Diol metabolite levels are expressed as a percentage of the sum of parent + diol peak areas.

protein concentration were assessed with the lowest substrate concentration later used in the substrate-saturation curves. No or negligible hydrolysis of oxetanes in compounds 1–3, 8, and 9 was observed in these preliminary assays, thus further kinetic experiments were only performed with compounds 4–7. From the second set of compounds 15 and 18 were selected for full kinetic characterization.

In assays with the recombinant enzyme, substrates (5–200 μM for compounds 5–7; 5–300 μM for compound 4; or 10–200 μM for compounds 15 and 18) were incubated with 1.9 $\mu\text{g}/\text{ml}$ (compounds 4–7) or 5.6 $\mu\text{g}/\text{ml}$ (compounds 15 and 18) of recombinant mEH, for either 10 minutes (compound 6), 30 minutes (compounds 5 and 7), 40 minutes (compound 4), or 60 minutes (compounds 15 and 18). The recombinant enzyme was thawed and diluted in cold Tris-HCl buffer (0.1 M, pH 9.0) supplemented with 0.1 mg/ml bovine serum albumin, which is necessary to stabilize the purified protein and help solubilize lipophilic substrates (Morisseau and Hammock, 2007). This mixture was preincubated at 37°C with constant shaking for 5 minutes, before starting the reactions with the addition of substrate (100 μl final reaction volume). An identical volume of substrate solution was added to each reaction directly from high-concentration acetonitrile stocks (compounds 4–7) or acetonitrile/DMSO stocks (compounds 15 and 18), to maintain the final solvent concentration $\leq 3\%$ (v/v) in all incubations. mEH activity has been reported to be unaffected by acetonitrile or DMSO concentrations up to 3% (v/v) (Seidegård and DePierre, 1980; Müller et al., 1997). Reactions were quenched and processed as described previously. All assays were performed in duplicate (compounds 4, 15, and 18) or triplicate (all other substrates), in round-bottom 96-well plates. To build calibration curves, synthetic diol standards 10–13, 21, and 22 (0.01–2.5 μM) were incubated, processed, and analyzed in the same manner as the substrates, except without enzyme.

Kinetic experiments with HLMs were performed similarly, but with the following exceptions: substrates (10–200 μM for compounds 5–7, 15, and 18 or 10–300 μM for compound 4) were incubated with 5 $\mu\text{g}/\text{ml}$ (compounds 4–7) or 15 $\mu\text{g}/\text{ml}$ (compounds 15 and 18) of HLM protein for 40 minutes (compounds 4–7) or 60 minutes (compounds 15 and 18), in sodium phosphate buffer (0.1 M, pH

7.4). Assays were performed in duplicate (compounds 7, 15, and 18) or triplicate (all other substrates) and the concentration range for calibration curves with synthetic diol standards was 0.1–5 μM . Under the conditions used, with no other metabolite formed than the ring-opened diol, substrate depletion did not exceed 6% with either enzyme system.

Determination of IC₅₀ for Inhibition of cSO Hydrolysis by VPD and Compounds 1–9. Human recombinant mEH was diluted to 1.9 $\mu\text{g}/\text{ml}$ in Tris-HCl buffer (0.1 M, pH 9.0) containing 0.1 mg/ml bovine serum albumin. Compounds 1–9 (0–200 μM) or VPD (0–2 mM) were added from acetonitrile stocks and the mixture was preincubated for 5 minutes at 37°C with constant shaking. Then, cSO was added from a DMSO stock to a final concentration equal to its K_m value (140 μM with the human recombinant enzyme) (Morisseau et al., 2011) and incubated for a further 10 minutes. Preliminary experiments confirmed a linear hydrobenzoin product formation in these conditions (data not shown). Final solvent concentrations were 0.56% DMSO and 2% acetonitrile in all incubations (100 μl total reaction volume). All assays were performed in triplicate in round-bottom 96-well plates. Generation of calibration curves and processing of the reactions were done as described in the previous section.

Metabolite Profiling and Data Analysis for Selective Inhibition Assays. For incubations with 1–9, 15–20, or 11,12-EET, UHPLC/Q-TOF analysis of metabolites from selective inhibition assays was performed as described previously (Li et al., 2016), with the following modifications: a different gradient profile was used with the initial mobile phase (90:10 A:B) transitioning to 70:30 A:B over 6 minutes and the mass spectrometer was a Synapt G2 Q-TOF (Waters (Milford, MA)). Mobile phase A was 0.1% formic acid in water (for reactions with oxetanes or 11,12-EET) or water (for reactions with cSO) and mobile phase B was acetonitrile. An MS^E method with two separate scan functions programmed with independent collision energies was used for data acquisition. Trap collision energy in function 1 was 4 V and in function 2 an energy ramp of 15–35 V was used; the transfer cell collision energy was 20 V. The entire system was operated using MassLynx (Waters, version 4.1), and data were processed with MetaboLynx version 4.1. MS and MS^E spectra were compared between the parent

compound and metabolites to identify metabolite structures and site(s) of modification in the substrate molecule. UHPLC/Q-TOF MS^E characteristics of compounds 1–9 and their hydrated metabolites are listed in Supplemental Table 1, although no MS^E spectra could be obtained for compounds 15–20. Products from reactions with cSO were analyzed by UV detection. The UHPLC eluate was introduced into an Acquity UV-PDA detector (Waters), and the diol hydrobenzoin metabolite in the experimental samples was identified by comparing the retention time with that of the authentic standard. Retention times for hydrobenzoin and cSO were 3.27 and 5.38 minutes, respectively. Metabolite peaks on the trace from the full UV scan (210–400 nm) were integrated using the TargetLynx tool (Waters).

Peak areas were used for the relative quantification of diol metabolites in HLM incubations without NADPH (reported in Table 1), by calculating

$$\text{Relative diol \%} = \frac{\text{Diol}_{\text{area}}}{\text{Diol}_{\text{area}} + \text{Parent}_{\text{area}}} \times 100$$

For incubations with inhibitors (or those lacking NADPH), relative diol levels were expressed as a percentage of the corresponding peak areas in control incubations with vehicle and NADPH.

Metabolite Quantification and Data Analysis for Kinetic Assays.

Chromatographic separation of metabolites from kinetic assays was performed on a Waters Acquity UHPLC HSS T3 column (2.1 × 100 mm, 1.8 μm for compounds 4–7) or a Waters Acquity UHPLC BEH column (2.1 × 100 mm, 1.7 μm for compounds 15 and 18) operated by an Acquity UHPLC system. To improve the separation between diols and parent compounds, mobile phase A was changed from 0.1% aqueous formic acid to 10 mM ammonium acetate in water; mobile phase B was acetonitrile. The initial mobile phase was 90:10 A:B, transitioning to 10:90 A:B over 6 minutes using a linear gradient, with a 7.7-minute total run time. The flow rate was 0.5 ml/min and the column oven was set to 45°C. A 1-minute window of UHPLC eluate, centered on the retention time of each diol metabolite, was introduced into a Xevo G2-S Q-TOF mass spectrometer for compounds 4–7 (Waters) or a Synapt G2 Q-TOF for compounds 15 and 18 (Waters), operating as described previously. Diols formed in incubations with compounds 4–8, 15, and 18 were quantified by external calibration as described in the previous sections, using TargetLynx (Waters). The extracted ion chromatograms corresponding to the protonated molecular ion of the diol were generated with a mass tolerance of 30 mDa.

To determine the K_m and V_{max} values, initial velocities were plotted versus the corresponding substrate concentration and fitted to the Michaelis-Menten equation by nonlinear regression, using GraphPad Prism version 6.07 for Windows (GraphPad Software, La Jolla, CA). Detection and quantification of hydrobenzoin formed in IC₅₀ assays with cSO was performed by UHPLC/UV as described in the previous section, except that 10 mM ammonium acetate was used as mobile phase A instead of water to avoid coelution of hydrobenzoin with oxetanes or diols. Velocities of hydrobenzoin formation were plotted against the logarithm of the corresponding inhibitor concentration and fitted to the one-site competitive binding equation by nonlinear regression, using GraphPad Prism.

Calculations of Ring-Strain Energies and Determination of p*K*_a. A detailed account of ring-strain energy calculations for relevant truncated fragments of compounds 1–9 is given in the Supplemental Material. Determination of solubility and log D for all oxetanes, and p*K*_a values for compounds 1–9 was performed as described previously (Boström et al., 2012).

Results

Oxetanes Are Opened Exclusively via Hydrolysis by mEH.

Compounds 1–9, 15–20, cSO, and 11,12-EET were incubated with human liver subcellular fractions or hepatocytes in the presence or absence of inhibitors of P450s, mEH, and sEH. Ring opening of the substrates in incubations with liver fractions was also monitored with or without NADPH. All oxetanes were metabolized to a variety of products in the presence of NADPH (see Fig. 1A for an example with compound 5 incubated with HLMs). Metabolites included products with a mass increase of 18 Da (H₂O) with respect to substrate and its *N*- or *O*-demethylation products.

The oxetanylmethylaminy moiety was the only part of each compound not retained in any of the fragment ions detected under the MS^E conditions used, and no fragment of the hydrated metabolite showed a mass shift of +18 Da relative to that of the parent (see representative MS and MS^E spectra for compound 5 in Fig. 2 and MS and MS^E data for all compounds in Supplemental Table 1). The hydrated metabolites formed from each parent compound were then found to coelute with the corresponding synthesized diols (see Fig. 1B for

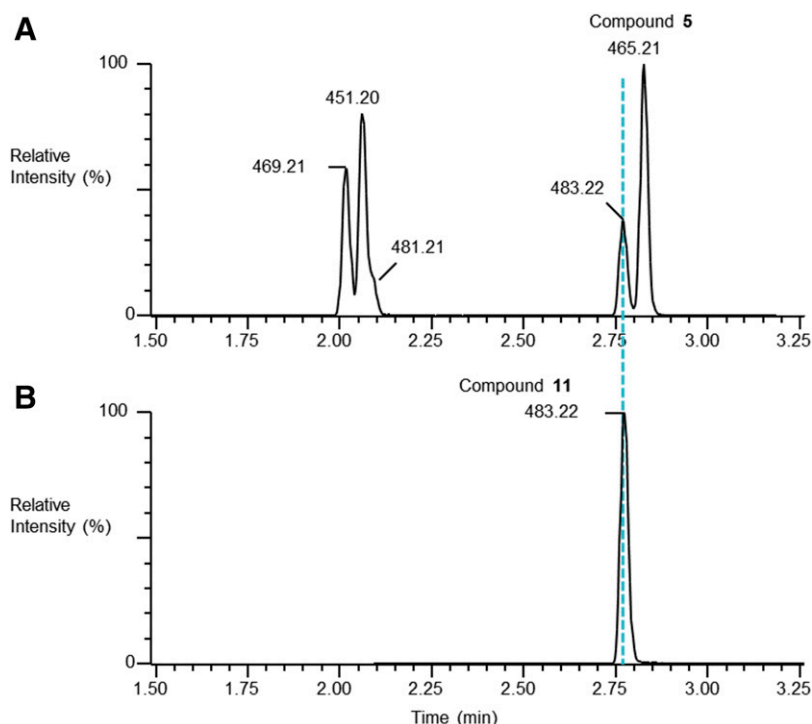


Fig. 1. Metabolism of compound 5. UHPLC-MS extracted ion chromatograms are shown for (A) compound 5 and its metabolites formed after 60-minute incubation with HLMs and NADPH and (B) synthetic diol 11. Peak labels are *m/z* values and correspond to parent (*m/z* 465.21), hydrolysis (*m/z* 483.22), oxidation (*m/z* 481.21), demethylation (*m/z* 451.20), and hydrolysis plus demethylation (*m/z* 469.21).

representative chromatograms for compound 5 and Supplemental Fig. 5 for the synthetic diol structures), and MS^E spectra of each metabolite/synthetic diol pair were identical (Fig. 2).

Hydration (addition of the elements of H₂O) for all test compounds was NADPH independent in incubations with HLMs (see Fig. 3 for an example with compound 6 and Supplemental Fig. 2 for all other compounds). In contrast, the formation of diols from all oxetanes and the mEH probe substrate cSO, but not from the sEH probe substrate 11,12-EET, was essentially abolished in the presence of high concentrations of the mEH inhibitor VPD in liver fractions and hepatocytes (Fig. 3; Supplemental Fig. 2). Similar results were obtained with the structurally unrelated mEH inhibitor PRG (data not shown). High concentrations of the P450 inhibitors KTZ and 1-ABT did not inhibit hydration of any compound (Fig. 3; Supplemental Fig. 2), while they greatly decreased demethylation of compounds 1, 3, 5–7, 9, and 15–20 (data not shown), indicating that a functional P450 system was present and could be effectively inhibited in the assay conditions used. Some degree of inhibition of diol formation by P450 inhibitors was observed for a compounds 4 and 15–17 in HLMs and 2, 5, 8, 16, and 17 in hepatocytes (Supplemental Fig. 2), but this was also observed for hydrolysis of the mEH probe substrate cSO (Supplemental Fig. 2). In addition, incubation of these and the other oxetanes with both NADPH and VPD completely abolished diol formation (Fig. 3; Supplemental Fig. 2). These data suggested that the apparent reduction of oxetane hydrolysis by P450 inhibitors for these compounds was likely due to experimental variation between samples, rather than a true contribution of P450s to oxetane ring opening. Conversely, diol formation from other compounds (1–3, 6, 7, and 15–18 in HLMs and 3, 4, 6, 7, and 9 in hepatocytes) increased in the absence of a functional P450 system (i.e., either in incubations without NADPH or in the presence of KTZ or 1-ABT) (Fig. 3; Supplemental

Fig. 2), while formation of the demethylated metabolites increased when mEH was inhibited (data not shown). Thus, inhibition of P450, or lack of NADPH, increased the availability of substrate for mEH-mediated metabolism, and conversely, inhibition of mEH increased substrate availability for P450-mediated metabolism. This indicated an apparent competition between mEH and P450s for the substrate and a lack of nonspecific inhibition of P450 activity by mEH inhibitors. Coincubation with the sEH inhibitor *t*-AUCB failed to inhibit hydration of oxetanes and cSO in hepatocytes (Fig. 3; Supplemental Fig. 2), whereas it abolished hydrolysis of the sEH probe substrate 11,12-EET in HLC (Supplemental Fig. 2). The same pattern of inhibition of oxetane hydration seen in HLMs and hepatocytes by VPD was also observed in HLC, where minor NADPH-independent diol formation occurred (Fig. 3; Supplemental Fig. 2). This is likely due to low levels of mEH contamination in the cytosol, as previously reported (Gill et al., 1982, 1983b). No diol formation was observed when the enzyme source was omitted (Fig. 3; Supplemental Fig. 2). The inhibitory profile seen with the selective epoxide hydrolase (EH) inhibitors VPD and *t*-AUCB against hydrolysis of the probe substrates cSO and 11,12-EET indicated that the assay was specific and effective at differentiating between metabolism catalyzed by the two forms of human EH.

Specific Structural Elements Modulate Oxetane Hydrolysis in HLMs and Hepatocytes. The oxetane substrates were hydrolyzed to varying degrees by mEH (Tables 1 and 2). Diol formation was absent or minor for compounds 1–3, 9, and 15–20, but was a major metabolic route for compounds 4–8. Among the full-length analogs, poor (1–3 and 9) and good (4–8) oxetane substrates also had significantly different pK_a values (6.5 ± 0.2 and 8.2 ± 0.1, respectively; *P* < 0.001, two-tailed unpaired T test) (Table 1), although they had similar solubilities, lipophilicities (Table 1), and theoretical ring-strain energies

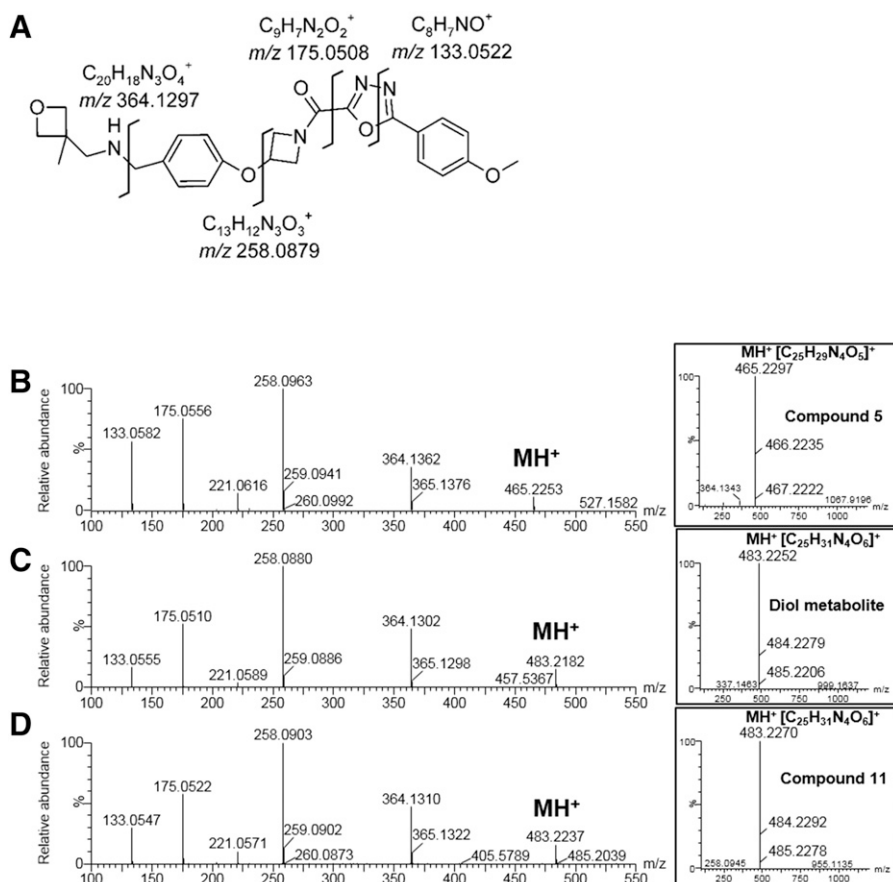


Fig. 2. Tentative fragmentation pattern (A) and MS^E spectra of compound 5 (B), its diol metabolite formed in incubations with HLMs (C) and the synthesized diol 11 (D). Insets are full-scan MS spectra.

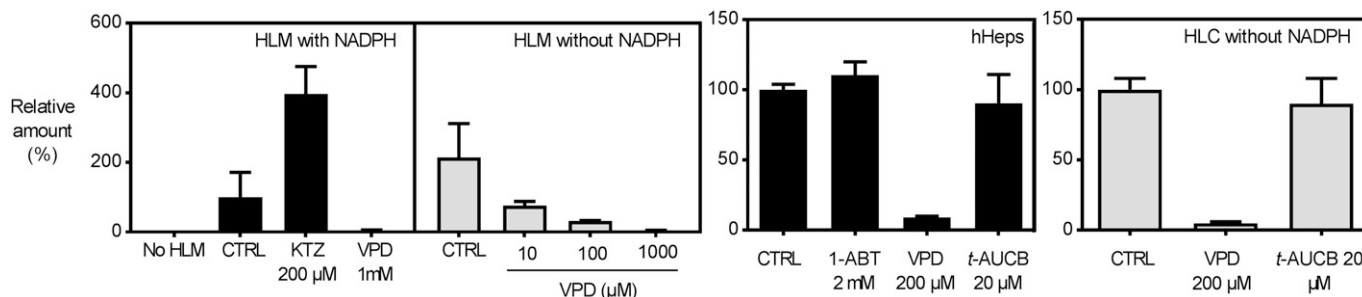


Fig. 3. Effect of P450 inhibitors KTZ and 1-ABT, the mEH inhibitor VPD and the sEH inhibitor *t*-AUCB (20 μM) on the hydration of compound 6 for HLMs, human hepatocytes (hHeps), and HLC. Assay conditions were: 10 μM substrate, 60-minute incubation with 1 mg/ml HLM or HLC protein; and 4 μM substrate, 2-hour incubation with 10⁶ hepatocytes/ml. Results are expressed as a % of the diol formed in reactions with NADPH and no inhibitor (CTRL), and bars are averages of duplicate measurements + range. Similar results were also obtained with the mEH inhibitor progabide.

(Supplemental Table 2). However, this trend in pK_a was not observed for the chain-shortened analogs (15–20), which showed broadly similar calculated pK_a values (Table 2).

Human Recombinant mEH Hydrolyses Oxetanes with the Same Substrate Preference as HLMs. To more fully understand the interaction of mEH with oxetanes, kinetic parameters for the hydrolysis of each of the full-length analogs (1–9) and two of the chain-shortened analogs (15 and 18) were determined in separate incubations with human recombinant mEH or HLMs. Among full-length compounds 1–9, both enzyme systems showed the same substrate preference and only efficiently hydrolyzed compounds 4–7. All four compounds 4–7 exhibited Michaelis-Menten-type kinetics with both the recombinant enzyme and HLM and showed similar K_m values (substrate-saturation curves are shown in Supplemental Figs. 3 and 4; Table 3). Hydrolysis of compounds 15 and 18 was less efficient and meant that K_m and V_{max} could only be determined with HLMs since within the substrate concentration range chosen the velocity remained linear with the recombinant enzyme (Supplemental Figs. 3 and 4; Table 3). No inhibition of *c*SO metabolism by compounds 1–9 was observed with recombinant mEH when using a substrate concentration corresponding to its K_m (data not shown). VPD, when tested under the same conditions, inhibited *c*SO hydrolysis with an IC_{50} value of $7.1 \pm 0.3 \mu M$.

Discussion

Oxetanes are being increasingly incorporated into the design of novel biologically active molecules (Wuitschik et al., 2010; Bull et al., 2016),

yet there are few detailed reports on their biotransformation. Here, we have shown that the oxetane moiety in a series of analogs can be consistently metabolized to a diol metabolite via hydrolysis by mEH, without contributions by any other enzyme system, and that this pathway may represent a major metabolic route depending on the structural context in which the oxetane is embedded. Oxetane rings thus represent a new class of substrates for human mEH.

An earlier study by Stepan et al. (2011) was the first to report metabolic ring cleavage of oxetanyl moieties in HLMs, but it was unclear which enzyme specifically catalyzed the formation of diol metabolites. A more recent study described an example of an oxetane-containing drug, EPZ015666, where the oxetanyl moiety was directly attached to a bicyclic aromatic core (Rioux et al., 2016). This compound was found to undergo ring opening to diol via P450-mediated oxidation, likely via α -hydroxylation, ring opening to the aldehyde, and finally reduction to diol (Rioux et al., 2016). This is in contrast to our recent (Li et al., 2016) and current findings and suggests that the environment of the oxetanyl moiety is a key to determining the metabolic fate of this class of compounds.

In the series of analogs analyzed in this study, altering the structural elements in the vicinity of the oxetane greatly affected the efficiency of hydrolytic ring cleavage by mEH. Seven compounds were studied initially (1–7), of which four (4–7) showed more than 10% hydrolysis. While these data are semiquantitative, not taking the potentially different MS response between the diols and corresponding parent into account, they served the purpose of dividing the compounds into two groups:

TABLE 3
Kinetic parameters for dihydrodiol formation in reactions with compounds 4–7, 15, and 18^a

Compound	Human Recombinant mEH			HLM without NADPH		
	K_m	V_{max}	V_{max}/K_m	K_m	V_{max}	V_{max}/K_m
	μM	$nmol/min/mg$		μM	$nmol/min/mg$	
4	67 ± 10	17 ± 1	0.26	27 ± 5	1.7 ± 0.1	0.06
5	47 (43, 59)	17 (17, 17)	0.36	26 ± 6	1.7 ± 0.1	0.07
6	89 ± 14	22 ± 2	0.24	28 ± 8	6.6 ± 0.7	0.27
7	50 ± 7	35 ± 2	0.69	51 (48, 56)	16 (15, 16)	0.31
15	^b	^b	^b	352 (239, 695)	0.9 (0.8, 1.4)	0.003
18	684 (650, 722)	2.8 (2.7, 3.0)	0.004	139 (119, 165)	0.4 (0.3, 0.4)	0.003
<i>c</i> SO ^c	141	570	4	7–25	17–52	2.1–2.5
SO ^d	^e	^e	^e	40–300	10–25	0.05–0.4

SO, styrene oxide.

^aValues are the mean of triplicates ± S.E., except for compounds 5, 15, and 18 incubated with recombinant mEH and compounds 7, 15, and 18 incubated with HLMs, for which the duplicate averages (replicate 1, replicate 2) are reported. Product formation was linear with respect to time and enzyme concentration.

^bKinetic parameters could not be estimated since the velocity remained linear within the substrate concentration range chosen.

^cValues are from Kitteringham et al. (1996), Hosagrahara et al. (2004), and Morisseau et al. (2011).

^dValues are from Seidegård and DePierre (1980), Pacifici et al. (1986), and Eugster et al. (1991).

^eNot tested

poor (1–3) and good (4–7) mEH substrates. This grouping was later supported when the compounds were tested with recombinant mEH. Two structural elements were present only in the compounds (4–7) most prone to hydrolysis, but were lacking from the others: 3-methyl substitution on the oxetane ring and a methylene group between the oxetane ring and the benzylic nitrogen. Two additional analogs were then synthesized, each containing only one of these structural elements (compounds 8 and 9). Addition of the 3-methyl substitution on the oxetane ring (compound 9) led to traces of diol formation, whereas introduction of a methylene spacer between the oxetane and the basic nitrogen (compound 8) led to an almost 2-fold increase in diol formed from the similarly substituted oxetane 3. This indicated that hydrolysis could be improved by the presence of a methylene spacer (compound 8 versus 3). Methyl substitutions alone, whether on oxetane (9) or benzylic nitrogen (1), do not affect hydrolysis, but in combination with the methylene spacer (4–7) each methyl substitution leads to a 5-fold increase in hydrolysis. To build on these initial structure-metabolism observations and to confirm that the specific enzymology of oxetane hydrolysis was retained with a minimal oxetane-containing substrate, a set of chain-shortened analogs was synthesized with masses ranging from 221 to 318 Da (15–20) (as outlined in the Supplemental Material). Specifically, the new set of compounds were analogs of compounds 4–8, where the 4-methoxyphenyl-oxadiazole amide-linked azetidine moiety had been replaced with a methyl group on the central phenyl ring. One analog (17) was prepared in which the 4-methoxyphenyl-oxadiazole was replaced with an acetoxy substitution on the central azetidine.

While hydrolysis was less efficient than that of the full-length analogs, most likely due to the lower lipophilicities of compounds 15–20, the chain-shortened analogs were still exclusively hydrolyzed by mEH, with no contributions from either P450s or sEH. A higher rate of hydrolysis of compounds 15–20 was observed with increasing methylation, as observed with the full-length analogs, whereas the presence of a methylene spacer between the amine and the phenyl ring decreased it.

When physicochemical parameters were considered as potential predictors of hydrolysis rate, it was initially observed that among full-length analogs 1–9, good mEH substrates (4–8) had significantly higher pK_a values; however, this did not apply to the set of chain-shortened compounds 15–20, which had calculated pK_a values similar to those of compounds 4–8 despite being hydrolyzed at a considerably lower rate. Similarly, no trends in solubility, lipophilicity, or calculated ring-strain energy was observed between good and poor substrates, indicating that hydrolysis efficiencies are likely determined by active site binding properties.

Importantly, the current work presents the first direct evidence of mEH-catalyzed oxetane hydrolysis with recombinant human mEH, which hydrolyzed oxetanes with the same substrate preference as human liver mEH. Kinetic experiments showed some variation in clearance (V_{max}/K_m) between substrates, and when compared with that of mEH probe substrates, oxetane clearance was lower than that for *c*SO, but similar to, or higher than that of styrene oxide (for reactions with HLMs) (Seidegård and DePierre, 1980; Pacifici et al., 1986; Eugster et al., 1991). Low K_m values and reaction rates are common for EHs, with turnover numbers for mEH substrates usually being lower than 1 second^{-1} (Oesch et al., 2000). This can be explained by the reported two-step catalytic mechanism for EHs: 1) the substrate rapidly binds to the active site forming a Michaelis complex, which then reversibly alkylates the enzyme forming an ester intermediate, and 2) this intermediate then undergoes hydrolysis to form the corresponding diol (Armstrong, 1999); for a schematic illustrating reaction of a spiro-oxetane substrate with mEH, see Li et al. (2016). The alkylation of the enzyme proceeds at a much faster rate (~ 3 orders of magnitude faster) than the hydrolysis of the ester bond (Tzeng et al., 1996), resulting in an accumulation of the ester intermediate and a low rate of product

formation (Oesch et al., 2000); therefore, low K_m values have been suggested to reflect a high degree of enzyme alkylation rather than a high affinity for the enzyme active site (Tzeng et al., 1996). Low rates of product formation thus do not necessarily reflect low efficiency of substrate consumption since the enzyme may bind more substrate than it forms diol (Oesch et al., 2000). Additionally, where mEH is highly expressed, e.g., in human liver (Thomas et al., 1982; de Waziers et al., 1990; Song et al., 2015), its concentration may exceed that of the substrate and thus substrate depletion *in vivo* may be more efficient than what is suggested by *in vitro* kinetic profiles. Nonetheless, the kinetic parameters evaluated according to the Michaelis-Menten model provide a means to compare the test compounds and their propensity to undergo hydrolysis by mEH. The name of the studied enzyme implies that only epoxides are accepted substrates and therefore our findings on the broader substrate specificity should motivate a change in enzyme description (EC 3.3.2.9) to include additional small strained ring systems, i.e., oxetanes.

In conclusion, we describe the enzyme-catalyzed hydrolysis of a series of simple oxetanes by mEH. The structural requirements for these oxetanyl-containing compounds to be accepted as substrates and hydrolyzed by mEH efficiently were characterized and the contributions from other enzymes were evaluated. These findings will be of value to medicinal chemists designing new oxetane-containing drug candidates. For example, it is not unusual that the metabolic clearance of an investigational drug is highly dependent on, e.g., CYP3A4, increasing the risk of drug-drug interactions with comedications. Introducing an oxetane into a chemistry series may be used as a tool to direct metabolism toward mEH and decrease the dependence on P450 metabolism. The degree to which this clearance route is tuned in or out can be adjusted using the structural modifications described herein.

This work describes the first stable, nonreactive class of substrates for human mEH, which will allow the reliable measurement of mEH enzyme activity in humans and the scaling from preclinical animal species to man. Finally, one can also envision exploitation of mEH as a biocatalyst for racemic oxetane resolution, in a similar manner to the use of, e.g., microbial and fungal EHs with epoxides (Hechtberger et al., 1993; Steinreiber and Faber, 2001; Widersten et al., 2010). The structure-metabolism relationship between strained ring-containing drug candidates and mEH is being further explored in ongoing studies on compounds with diverse scaffolds.

Acknowledgments

The authors thank Dr. Bruce Hammock and Dr. Christophe Morisseau (University of California Davis, Davis, CA) for the generous gift of the recombinant enzyme, Dr. Sten Nilsson-Lill (AstraZeneca) for helpful discussions on computational methods, and Dr. Neal Castagnoli Jr. (Virginia Tech, Blacksburg, VA) and Dr. Erick Carreira (ETH Zurich, Zürich, Switzerland) for helpful discussions and critical reading of the manuscript.

Authorship Contributions

Participated in research design: Toselli, Li, Johansson, Weidolf, Hayes.
Conducted experiments: Toselli, Fredenwall.
Contributed new reagents or analytic tools: Svensson.
Performed data analysis: Toselli, Fredenwall, Svensson, Li, Johansson, Weidolf, Hayes.
Wrote or contributed to the writing of the manuscript: Toselli, Fredenwall, Svensson, Li, Johansson, Weidolf, Hayes.

References

- Armstrong RN (1999) Kinetic and chemical mechanism of epoxide hydrolase. *Drug Metab Rev* **31**: 71–86.
- Boström J, Hogner A, Llinàs A, Wellner E, and Plowright AT (2012) Oxadiazoles in medicinal chemistry. *J Med Chem* **55**:1817–1830.
- Bull JA, Croft RA, Davis OA, Doran R, and Morgan KF (2016) Oxetanes: recent advances in synthesis, reactivity, and medicinal chemistry. *Chem Rev* **116**:12150–12233.

- Chacos N, Capdevila J, Falck JR, Manna S, Martin-Wixtrom C, Gill SS, Hammock BD, and Estabrook RW (1983) The reaction of arachidonic acid epoxides (epoxyeicosatrienoic acids) with a cytosolic epoxide hydrolase. *Arch Biochem Biophys* **223**:639–648.
- de Waziers I, Cugnenc PH, Yang CS, Leroux JP, and Beaune PH (1990) Cytochrome P 450 isoenzymes, epoxide hydrolase and glutathione transferases in rat and human hepatic and extra-hepatic tissues. *J Pharmacol Exp Ther* **253**:387–394.
- Emoto C, Murase S, Sawada Y, Jones BC, and Iwasaki K (2003) In vitro inhibitory effect of 1-aminobenzotriazole on drug oxidations catalyzed by human cytochrome P450 enzymes: a comparison with SKF-525A and ketoconazole. *Drug Metab Pharmacokinet* **18**:287–295.
- Eugster HP, Sengstag C, Hinnen A, Meyer UA, and Würigler FE (1991) Heterologous expression of human microsomal epoxide hydrolase in *Saccharomyces cerevisiae*. Study of the valpromide-carbamazepine epoxide interaction. *Biochem Pharmacol* **42**:1367–1372.
- Gill SS, Ota K, and Hammock BD (1983a) Radiometric assays for mammalian epoxide hydrolases and glutathione S-transferase. *Anal Biochem* **131**:273–282.
- Gill SS, Ota K, Ruebner B, and Hammock BD (1983b) Microsomal and cytosolic epoxide hydrolases in rhesus monkey liver, and in normal and neoplastic human liver. *Life Sci* **32**:2693–2700.
- Gill SS, Wie SI, Guenther TM, Oesch F, and Hammock BD (1982) Rapid and sensitive enzyme-linked immunosorbent assay for the microsomal epoxide hydrolase. *Carcinogenesis* **3**:1307–1310.
- Hechtberger P, Wirnsberger G, Mischitz M, Klempier N, and Faber K (1993) Asymmetric hydrolysis of epoxides using an immobilized enzyme preparation from *Rhodococcus* sp. *Tetrahedron Asymmetry* **4**:1161–1164.
- Hosagrahara VP, Rettie AE, Hassett C, and Omiecinski CJ (2004) Functional analysis of human microsomal epoxide hydrolase genetic variants. *Chem Biol Interact* **150**:149–159.
- Johansson A, Löfberg C, Antonsson M, von Unge S, Hayes MA, Judkins R, Ploj K, Benthem L, Lindén D, Brodin P, et al. (2016) Discovery of (3-(4-(2-Oxa-6-azaspiro[3.3]heptan-6-ylmethyl)phenoxy)azetidin-1-yl)(5-(4-methoxyphenyl)-1,3,4-oxadiazol-2-yl)methanone (AZD1979), a melanin concentrating hormone receptor 1 (MCHR1) antagonist with favorable physicochemical properties. *J Med Chem* **59**:2497–2511.
- Kerr BM, Rettie AE, Eddy AC, Loiseau P, Guyot M, Wilensky AJ, and Levy RH (1989) Inhibition of human liver microsomal epoxide hydrolase by valproate and valpromide: in vitro/in vivo correlation. *Clin Pharmacol Ther* **46**:82–93.
- Kitteringham NR, Davis C, Howard N, Pirmohamed M, and Park BK (1996) Interindividual and interspecies variation in hepatic microsomal epoxide hydrolase activity: studies with *cis*-stilbene oxide, carbamazepine 10, 11-epoxide and naphthalene. *J Pharmacol Exp Ther* **278**:1018–1027.
- Kroetz DL, Loiseau P, Guyot M, and Levy RH (1993) In vivo and in vitro correlation of microsomal epoxide hydrolase inhibition by progabide. *Clin Pharmacol Ther* **54**:485–497.
- Li XQ, Hayes MA, Grönberg G, Berggren K, Castagnoli N, Jr, and Weidolf L (2016) Discovery of a novel microsomal epoxide hydrolase-catalyzed hydration of a spiro oxetane. *Drug Metab Dispos* **44**:1341–1348.
- Liu JY, Park SH, Morisseau C, Hwang SH, Hammock BD, and Weiss RH (2009) Sorafenib has soluble epoxide hydrolase inhibitory activity, which contributes to its effect profile in vivo. *Mol Cancer Ther* **8**:2193–2203.
- Morisseau C, Bernay M, Escaich A, Sanborn JR, Lango J, and Hammock BD (2011) Development of fluorescent substrates for microsomal epoxide hydrolase and application to inhibition studies. *Anal Biochem* **414**:154–162.
- Morisseau C and Hammock BD (2005) Epoxide hydrolases: mechanisms, inhibitor designs, and biological roles. *Annu Rev Pharmacol Toxicol* **45**:311–333.
- Morisseau C and Hammock BD (2007) Measurement of soluble epoxide hydrolase (sEH) activity, in *Curr Protoc Toxicol* **4**:4.23.1–4.23.18, Wiley Interscience, doi: 10.1002/0471140856.tx0423s33.
- Müller F, Arand M, Frank H, Seidel A, Hinz W, Winkler L, Hänel K, Blée E, Beetham JK, Hammock BD, et al. (1997) Visualization of a covalent intermediate between microsomal epoxide hydrolase, but not cholesterol epoxide hydrolase, and their substrates. *Eur J Biochem* **245**:490–496.
- Oesch F, Herrero ME, Hengstler JG, Lohmann M, and Arand M (2000) Metabolic detoxification: implications for thresholds. *Toxicol Pathol* **28**:382–387.
- Pacifici GM, Franchi M, Bencini C, and Rane A (1986) Valpromide inhibits human epoxide hydrolase. *Br J Clin Pharmacol* **22**:269–274.
- Rioux N, Duncan KW, Lantz RJ, Miao X, Chan-Penebre E, Moyer MP, Munchhof MJ, Copeland RA, Chesworth R, and Waters NJ (2016) Species differences in metabolism of EPZ015666, an oxetane-containing protein arginine methyltransferase-5 (PRMT5) inhibitor. *Xenobiotica* **46**:268–277.
- Seidegård J and DePierre JW (1980) Benzil, a potent activator of microsomal epoxide hydrolase in vitro. *Eur J Biochem* **112**:643–648.
- Song W, Yu L, and Peng Z (2015) Targeted label-free approach for quantification of epoxide hydrolase and glutathione transferases in microsomes. *Anal Biochem* **478**:8–13.
- Steinreiber A and Faber K (2001) Microbial epoxide hydrolases for preparative biotransformations. *Curr Opin Biotechnol* **12**:552–558.
- Stepan AF, Karki K, McDonald WS, Dorff PH, Dutra JK, Dirico KJ, Won A, Subramanyam C, Efremov IV, O'Donnell CJ, et al. (2011) Metabolism-directed design of oxetane-containing arylsulfonamide derivatives as γ -secretase inhibitors. *J Med Chem* **54**:7772–7783.
- Thomas PE, Ryan DE, von Bahr C, Glaumann H, and Levin W (1982) Human liver microsomal epoxide hydrolase. Correlation of immunochemical quantitation with catalytic activity. *Mol Pharmacol* **22**:190–195.
- Tzeng HF, Laughlin LT, Lin S, and Armstrong RN (1996) The catalytic mechanism of microsomal epoxide hydrolase involves reversible formation and rate-limiting hydrolysis of the alkyl-enzyme intermediate. *J Am Chem Soc* **118**:9436–9437.
- Václavíková R, Hughes DJ, and Souček P (2015) Microsomal epoxide hydrolase 1 (EPHX1): gene, structure, function, and role in human disease. *Gene* **571**:1–8.
- Widersten M, Gurell A, and Lindberg D (2010) Structure-function relationships of epoxide hydrolases and their potential use in biocatalysis. *Biochim Biophys Acta* **1800**:316–326.
- Wuitschik G, Carreira EM, Wagner B, Fischer H, Parrilla I, Schuler F, Rogers-Evans M, and Müller K (2010) Oxetanes in drug discovery: structural and synthetic insights. *J Med Chem* **53**:3227–3246.

Address correspondence to: Dr. Martin A. Hayes, Cardiovascular and Metabolic Diseases, Innovative Medicines and Early Development, AstraZeneca, Pepparedsleden 1, Mölndal, 431 83, Sweden. E-mail: martin.hayes@astrazeneca.com